



CHORUS

This is the accepted manuscript made available via CHORUS. The article has been published as:

Emulating Nonreciprocity with Spatially Dispersive Metasurfaces Excited at Oblique Incidence

Carl Pfeiffer and Anthony Grbic

Phys. Rev. Lett. **117**, 077401 — Published 10 August 2016

DOI: [10.1103/PhysRevLett.117.077401](https://doi.org/10.1103/PhysRevLett.117.077401)

Emulating Nonreciprocity with Spatially Dispersive Metasurfaces Excited at Oblique Incidence

Carl Pfeiffer and Anthony Grbic

Department of Electrical Engineering
University of Michigan
Ann Arbor, MI 48109-2122, USA
agrbic@umich.edu

Abstract— Ultra-thin metasurfaces supporting transverse surface currents provide extreme electromagnetic wavefront and polarization control. Here, it is shown that adding longitudinal (normal) surface currents significantly expands the scope of electromagnetic phenomena that can be engineered with reciprocal materials. In particular, these metasurfaces are inherently spatially dispersive, which allows them to emulate nonreciprocal phenomena. It is analytically shown that spatially dispersive metasurfaces are effectively self-biased using the transverse momentum of the incident wavefront. Longstanding notions of what makes a metasurface reciprocal are reinvestigated, and generalized reciprocity relations are derived. Several metasurfaces are designed that imitate Faraday rotation and optical isolation when illuminated with obliquely incident plane waves and normally incident vortex beams. These new surfaces break the inherent symmetry of previous metasurface designs, enabling low-profile devices with unprecedented functionality.

Keywords—*metasurface; metamaterial; polarizability; bianisotropic; optical vortex; spatial dispersion*

Nonreciprocal phenomena are at the heart of many optical and electronic devices. Although nonreciprocal devices can in general provide greater field control than reciprocal devices, they require either nonlinear materials [1], or a complicated biasing mechanism such as a static magnetic field [2], static electric field [3], or time-varying electric field [4, 5]. This has motivated the development of reciprocal devices that can mimic nonreciprocal effects. For example, an isolator is a common nonreciprocal component that provides unidirectional transmission, and protects an electromagnetic source from unwanted reflections. It is possible to emulate the response of an isolator using reciprocal materials with a so-called “poor man’s isolator.” A poor-man’s isolator consists of a linear polarizer followed by a quarter-wave plate [6]. It protects a source from reflections by exploiting the fact that a circularly polarized wave is converted to the orthogonal polarization (i.e. the handedness is switched) upon reflection from most objects.

Here, it is shown that spatial dispersion can be exploited to significantly expand the scope of electromagnetic phenomena that can be engineered with reciprocal materials. Photonic crystals and anisotropic materials, could in principle emulate the wide range of nonreciprocal phenomena that are discussed here [7-9]. However, the main challenge arises from the fact that it has been relatively difficult to engineer the spatial dispersion of these structures, which has motivated significant efforts to simply minimize it [10]. Therefore, metasurfaces are considered here, which significantly simplifies the analysis due to their reduced dimensionality. This allows a concise expression to be derived that relates spatial dispersion to 2D (tangential) surface parameters, which provides physical intuition. Furthermore, it is analytically shown that that the transverse momentum of an incident wave can effectively self-bias a spatially dispersive metasurface, and allow it to emulate nonreciprocal phenomena.

To begin, let us define the scattering parameters (S-parameters) of an arbitrary planar structure that is located in the $z = 0$ plane. Translation symmetry is assumed such that the reflected and transmitted waves are scattered to the specular directions (i.e. transverse momentum is conserved). In addition, the structure is surrounded by free space with wavenumber $k_0 = \omega\sqrt{\epsilon_0\mu_0}$ and wave impedance $\eta_0 = \sqrt{\mu_0/\epsilon_0}$. Without loss of generality, the structure is illuminated with a plane wave that is obliquely incident in the yz -plane with transverse wavenumber k_y and longitudinal wavenumber k_z , where $k_y^2 + k_z^2 = k_0^2$. The S-parameters are equal to the ratio of the scattered electric field to the incident electric field. In general,

$$\mathbf{S}_{nm} = \begin{pmatrix} S_{nm}^{TE,TE} & S_{nm}^{TE,TM} \\ S_{nm}^{TM,TE} & S_{nm}^{TM,TM} \end{pmatrix}, \quad (1)$$

is a 2×2 matrix relating the field scattered into region n when a plane wave is incident from region m . The superscript TE (TM) denotes an electric (magnetic) field that is polarized transverse to the plane of incidence (yz plane), as shown in Fig. 1. It is important to note that the scattering parameters are defined for a unique transverse wavenumber (k_y). Thus, waves incident from the region $z > 0$ propagate with transverse and longitudinal wavenumbers, k_y and $-k_z$, respectively.

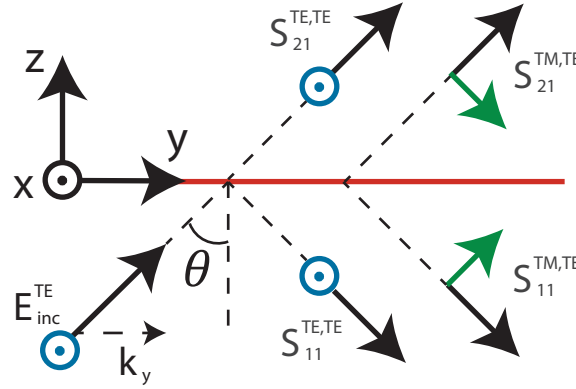


Fig. 1: Relevant scattering parameters when a TE polarized plane wave is obliquely incident from the region $z < 0$.

It is often stated that reciprocity requires $\mathbf{S} = \mathbf{S}^T$, where T denotes matrix transpose. However, this is only true at normal incidence. It can be easily verified that if an arbitrary structure is illuminated at oblique incidence, then reciprocity requires $\mathbf{S}(k_y) = \mathbf{S}(-k_y)^T$. Therefore, the transverse momentum (k_y) can be envisaged as a biasing mechanism that allows nonreciprocal effects to be emulated. When the wave is biased with a unique and nonzero transverse momentum (i.e. $k_y \neq 0$), reciprocity places no restrictions upon the scattering parameters that can be realized. Reciprocity only outlines the effect of flipping the bias direction. Although it is straightforward to show that it is theoretically possible to realize arbitrary scattering parameters at oblique incidence, a systematic method of designing these devices has not been reported. Here, it is shown that low symmetry metasurfaces provide a particularly simple and general approach for engineering the scattering parameters.

A metasurface can be envisaged as a boundary condition that relates the average electric and magnetic fields at the surface to the induced polarization surface currents [11, 12]. Bianisotropic metasurfaces supporting only transverse surface currents have demonstrated the ability to realize any wave transformation permitted by reciprocity when they are illuminated at normal incidence [13-15]. However, when the metasurface is illuminated at oblique incidence, adding out-of-plane surface currents allows nonreciprocal effects to be emulated. These metasurfaces are inherently spatially dispersive, even in the homogenous limit.

It should be noted that some metasurfaces supporting longitudinal polarization currents have been analyzed previously, but only under the conditions where there is significant symmetry [11, 16-18]. Specifically, the \mathbf{xz} , \mathbf{zx} , \mathbf{yz} and \mathbf{zy} dyads of previous surface parameters were always zero. Fundamentally new surface properties can be realized when these symmetry restrictions are relaxed.

As in Refs. [11, 13], a polarizable particle is distributed along a two-dimensional array in the $z = 0$ plane, and a time harmonic ($e^{j\omega t}$) excitation is assumed. For such an arrangement, the constituent surface parameters can be written as,

$$\begin{pmatrix} \mathbf{J}_s \\ \mathbf{M}_s \end{pmatrix} = \begin{pmatrix} \mathbf{Y} & \boldsymbol{\chi} \\ \boldsymbol{\kappa} & \mathbf{Z} \end{pmatrix} \begin{pmatrix} \mathbf{E}_{avg} \\ \mathbf{H}_{avg} \end{pmatrix}, \quad (2)$$

where \mathbf{J}_s and \mathbf{M}_s are 3D electric and magnetic surface currents, and \mathbf{E}_{avg} and \mathbf{H}_{avg} are average electric and magnetic fields at the surface. Intuitively, \mathbf{Y} and \mathbf{Z} are the time harmonic electric and magnetic surface susceptibilities, respectively. Similarly, $\boldsymbol{\chi}$ and $\boldsymbol{\kappa}$ are the time harmonic electro-magnetic and magneto-electric surface parameters. Since \mathbf{Y} , \mathbf{Z} , $\boldsymbol{\chi}$, and $\boldsymbol{\kappa}$ are each 3×3 matrices, they are referred to as the 3D surface parameters. If the surface is lossless and reciprocal: $\mathbf{Y} = \mathbf{Y}^T$, $\mathbf{Z} = \mathbf{Z}^T$, $\boldsymbol{\kappa} = -\boldsymbol{\chi}^T$, \mathbf{Y} and \mathbf{Z} are imaginary, $\boldsymbol{\chi}$ and $\boldsymbol{\kappa}$ are real [19]. In the homogenous limit (i.e. particle size and spacing are infinitely small), the 3D constituent surface parameters are fundamental in that they do not depend on the incident field (i.e. they are not spatially dispersive).

The fields on either side of the metasurface are related to the surface currents by [20],

$$\begin{aligned} \mathbf{z} \times \mathbf{H} \Big|_{z=0^-}^{0^+} &= \mathbf{J}_s^t - \mathbf{z} \times \nabla_t \frac{M_{sz}}{jk_0\eta_0} = \tilde{\mathbf{J}}_s^t, \\ \mathbf{E} \Big|_{z=0^-}^{0^+} \times \mathbf{z} &= \mathbf{M}_s^t + \mathbf{z} \times \nabla_t \frac{J_{sz}\eta_0}{jk_0} = \tilde{\mathbf{M}}_s^t, \end{aligned} \quad (3)$$

where t denotes tangent to the surface, and \mathbf{z} is a unit vector. Effective 2D surface currents $\tilde{\mathbf{J}}_s^t$ and $\tilde{\mathbf{M}}_s^t$ are also defined in (3), which model the combined effect of the tangential and longitudinal surface currents.

The scattering parameters can be directly related to the 3D surface parameters using (3). However, metasurfaces are most often modelled as structures that support only transverse polarization currents since the Equivalence Principle stipulates that an arbitrary object can be replaced by a unique set of transverse surface currents [21]. Therefore, it is informative to consider the case where the metasurface is modelled with 2D constituent surface parameters, $\tilde{\mathbf{Y}}$, $\tilde{\boldsymbol{\chi}}$, $\tilde{\boldsymbol{\kappa}}$, $\tilde{\mathbf{Z}}$, which are defined as,

$$\begin{pmatrix} \tilde{\mathbf{J}}_s^t \\ \tilde{\mathbf{M}}_s^t \end{pmatrix} = \begin{pmatrix} \tilde{\mathbf{Y}} & \tilde{\boldsymbol{\chi}} \\ \tilde{\boldsymbol{\kappa}} & \tilde{\mathbf{Z}} \end{pmatrix} \begin{pmatrix} \tilde{\mathbf{E}}_{avg}^t \\ \tilde{\mathbf{H}}_{avg}^t \end{pmatrix}. \quad (4)$$

The tilde is used here to indicate two-dimensional vectors and matrices. The 2D surface parameters are particularly useful since there exists a one-to-one relationship between the 2D surface parameters and the scattering parameters [13, 14]. In contrast, the 3D surface parameters cannot be uniquely determined from reflection/transmission measurements at a single angle of incidence, since there are an infinite number of 3D surface parameters that realize the same scattering parameters.

Inserting (2) and (4) into (3), and assuming a plane wave excitation, the 2D constituent surface parameters can be related to the 3D surface parameters as follows [22],

$$\begin{pmatrix} \tilde{\mathbf{Y}} & \tilde{\boldsymbol{\chi}} \\ \tilde{\boldsymbol{\kappa}} & \tilde{\mathbf{Z}} \end{pmatrix} = \begin{pmatrix} Y_{xx} + \frac{Z_{zz}k_y^2}{(k_0\eta_0)^2} - \frac{k_y(\chi_{xz} + \kappa_{zx})}{\eta_0 k_0} & Y_{xy} - \frac{k_y\kappa_{zy}}{k_0\eta_0} & \chi_{xx} - \frac{\kappa_{zz}k_y^2}{k_0^2} + \frac{k_y(Y_{xz}\eta_0 - \frac{Z_{zx}}{\eta_0})}{k_0} & \chi_{xy} - \frac{k_y Z_{zy}}{k_0\eta_0} \\ Y_{yx} - \frac{k_y\chi_{yz}}{k_0\eta_0} & Y_{yy} & \chi_{yx} + \frac{k_y\eta_0 Y_{yz}}{k_0} & \chi_{yy} \\ \kappa_{xx} - \frac{\chi_{zz}k_y^2}{k_0^2} + \frac{k_y(Y_{zx}\eta_0 - \frac{Z_{xz}}{\eta_0})}{k_0} & \kappa_{xy} + \frac{k_y\eta_0 Y_{zy}}{k_0} & Z_{xx} + \frac{Y_{zz}(k_y\eta_0)^2}{k_0^2} + \frac{k_y(\chi_{zx} + \kappa_{xz})}{\eta_0 k_0} & Z_{xy} + \frac{k_y\eta_0 \chi_{zy}}{k_0} \\ \kappa_{yx} - \frac{k_y Z_{yz}}{k_0\eta_0} & \kappa_{yy} & Z_{yx} + \frac{k_y\eta_0 \kappa_{yz}}{k_0} & Z_{yy} \end{pmatrix}. \quad (5)$$

Several conclusions can be drawn from (5). In contrast to the 3D surface parameters, the 2D surface parameters depend upon the transverse wavenumber of the incident field, k_y [23]. Therefore the metasurface is inherently spatially dispersive when it supports longitudinal polarization currents. When the metasurface is illuminated with a normally incident plane wave (i.e. $k_y = 0$), the 3D and 2D surface parameters are equivalent. For arbitrary angles of incidence, the 2D surface parameters of a lossless and reciprocal metasurface satisfy the standard lossless constraints: $\tilde{\mathbf{Y}} = -\tilde{\mathbf{Y}}^\dagger$, $\tilde{\mathbf{Z}} = -\tilde{\mathbf{Z}}^\dagger$, $\tilde{\boldsymbol{\kappa}} = -\tilde{\boldsymbol{\chi}}^\dagger$, where \dagger denotes transpose and complex conjugate. However, the 2D surface parameters do not in general satisfy the standard reciprocity constraints: $\tilde{\mathbf{Y}} \neq \tilde{\mathbf{Y}}^T$, $\tilde{\mathbf{Z}} \neq \tilde{\mathbf{Z}}^T$, $\tilde{\boldsymbol{\kappa}} \neq -\tilde{\boldsymbol{\chi}}^T$ when the metasurface supports out-of-plane surface currents [13, 24-27]. In other words, $\mathbf{S} \neq \mathbf{S}^T$ for oblique incidence. Previous derivations of metasurface reciprocity implicitly assumed the 2D surface parameters are not spatially dispersive [24], which is not the case here. A derivation providing generalized reciprocity conditions that properly account for spatial dispersion is provided in the Supplemental Material [22]. The 2D surface parameters in (5) satisfy these updated reciprocity conditions: $\tilde{\mathbf{Y}}(k_y) = \tilde{\mathbf{Y}}^T(-k_y)$, $\tilde{\mathbf{Z}}(k_y) = \tilde{\mathbf{Z}}^T(-k_y)$, $\tilde{\boldsymbol{\kappa}}(k_y) = -\tilde{\boldsymbol{\chi}}^T(-k_y)$. This is equivalent to stating that time reversal symmetry is satisfied by the metasurface. Therefore, it should be emphasized that nonreciprocal devices which break time-reversal symmetry cannot be realized with spatially dispersive metasurfaces. However, there remain many applications that could benefit from passive structures that merely imitate, rather than reproduce, nonreciprocal phenomena.

Next, three different metasurfaces supporting out-of-plane surface currents are introduced. Each metasurface is designed to mimic the response of a well-known optical device that uses nonreciprocal materials. However, the metasurfaces are in fact reciprocal even though they do not satisfy the previously stated reciprocity conditions (i.e. symmetric 2D surface parameters). Detailed dimensions, as well as additional simulations and measurements are provided in the Supplemental Material for each design [22]. Note that the Supplemental Material also includes Ref. [28].

First, Faraday rotation is emulated. Faraday rotation is the basis behind many nonreciprocal devices, such as circulators and isolators. The Faraday effect causes the polarization of light to rotate as it propagates through a magneto-optical material biased with a static magnetic field B_0 in the direction of propagation. The magneto-optical material is usually modelled with an asymmetric permittivity tensor: $\boldsymbol{\varepsilon} = \begin{pmatrix} \varepsilon_{xx} & j\gamma B_0 \\ -j\gamma B_0 & \varepsilon_{yy} \end{pmatrix}$, where γ is the magnetogyration coefficient responsible for polarization rotation [29]. Faraday rotation is distinct from optical activity since the handedness of Faraday rotation is the same when propagating in the $+\mathbf{z}$ and $-\mathbf{z}$ directions. A simple method of distinguishing optical activity from Faraday rotation is to back a material under consideration with a metallic plane, and observe the reflected polarization. Conventional wisdom suggests that only nonreciprocal materials can rotate an arbitrary incident polarization upon reflection. However, inspection of (5) reveals that the 2D electric response ($\tilde{\mathbf{Y}}$) is also asymmetric when the metasurface is comprised of reciprocal materials with nonzero magneto-electric coupling ($\chi_{yz} = -\kappa_{zy} \neq 0$). This has exactly the same form as the permittivity of a magneto-optical material, but with the magnetic bias

(B_0) replaced with the transverse momentum of the incident wave (k_y), and the magnetogyration coefficient (γ) replaced with the magneto-electric coupling ($\chi_{yz} = -\kappa_{zy}$). Therefore, the transverse momentum provides a self-biasing mechanism since the spatially dispersive metasurface is biased by the incident wave itself.

A metasurface was designed to rotate an obliquely incident plane wave with arbitrary incident polarization by 90° upon reflection: $\mathbf{S}_{11} = e^{j\phi} \begin{pmatrix} 0 & 1 \\ -1 & 0 \end{pmatrix}$. The metasurface geometry and performance are shown in Fig. 2. The split-ring-resonator couples a \mathbf{z} -directed magnetic field to a \mathbf{y} -directed electric current (χ_{yz}), and a \mathbf{y} -directed electric field to a \mathbf{z} -directed magnetic current (κ_{zy}). When illuminated with a plane wave with angle of incidence $\theta = 45^\circ$ ($k_y/k_0 = k_z/k_0 = 1/\sqrt{2}$), the simulated reflection coefficient of the unit cell is $\mathbf{S}_{11} = e^{2.57j} \begin{pmatrix} -0.05 + 0.01j & 0.94 - 0.00j \\ -0.94 - 0.04j & -0.01 - 0.02j \end{pmatrix}$, at the operating frequency of 10 GHz. When the incident polarization is linear, the measured cross-polarized (rotated) reflectance is above 80% and the co-polarized reflectance is below 2%, independent of the orientation of the incident polarization. Therefore, the metasurface acts as a near-ideal polarization rotator.

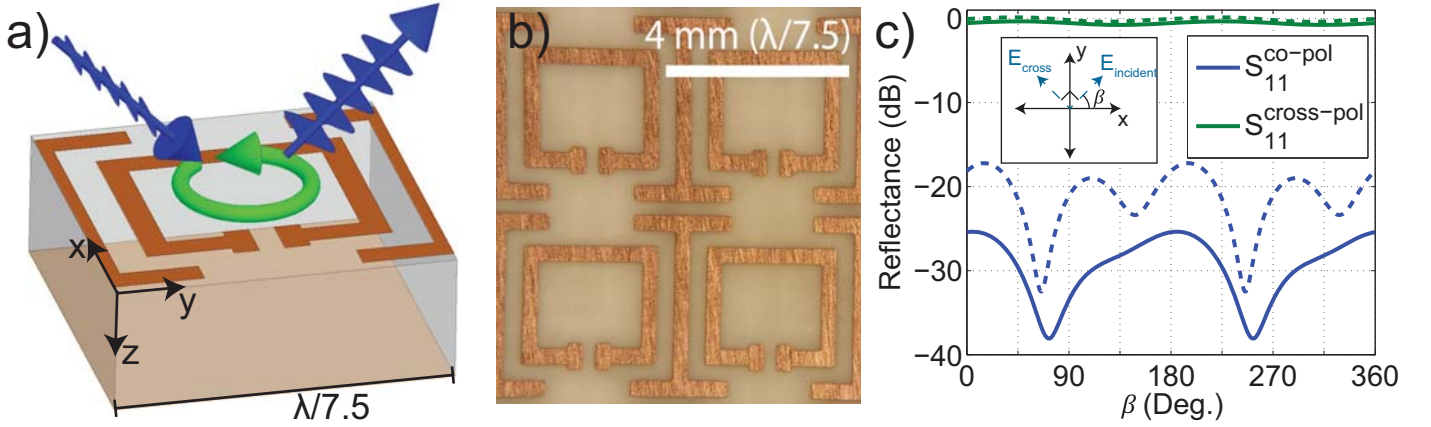


Fig. 2: Three-dimensional metasurface emulating Faraday rotation. (a) The metasurface rotates an arbitrary incident polarization by 90° upon reflection. (b) Fabricated metasurface that operates at 10 GHz. (c) Co- and cross-polarized reflection when illuminated with linearly polarized plane waves with electric field oriented at an angle β from the x -axis. Solid and dashed lines correspond to simulations and measurements, respectively.

Next, a metasurface providing unidirectional transmission is designed, which emulates the response of a nonreciprocal isolator. Isolators provide high transmission in the $+\mathbf{z}$ direction and high absorption in the $-\mathbf{z}$ direction, which protects devices in the region $z < 0$ from reflections originating from objects in the region $z > 0$ [29]. An ideal isolator is polarization independent, has $\mathbf{S}_{11} = \mathbf{S}_{22} = \mathbf{S}_{12} = \mathbf{0}$, and $\mathbf{S}_{21} = \begin{pmatrix} 1 & 0 \\ 0 & 1 \end{pmatrix}$. From the stipulated S-parameters, it can be shown that the necessary 3D surface parameters are given by:

$$\begin{aligned} \eta_0 Y_{yy} &= Z_{yy}/\eta_0 = k_0/k_z, \\ \eta_0 Y_{zz} &= Z_{zz}/\eta_0 = k_0 k_z/k_y^2, \\ \eta_0 Y_{yz} &= \eta_0 Y_{zy} = Z_{yz}/\eta_0 = Z_{zy}/\eta_0 = k_0/k_y, \end{aligned} \tag{6}$$

and all other terms are 0 [22]. In other words, the metasurface should provide identical, anisotropic electric and magnetic responses that are lossy. A metasurface providing unidirectional transmission that is designed to work for $\theta = 45^\circ$ at 10 GHz is shown in Fig. 3. The electric response is generated using electric dipoles centrally loaded with an inductor (8.15 nH) and resistor (18.8 Ω) in series, which forms a lossy resonator. The magnetic response is generated with loops that surround the dipoles. Each loop is symmetrically loaded with four capacitors (0.152 pF) and resistors (3.75 Ω). The simulated transmittance in the $+z$ direction ($|S_{21}|^2$) and $-z$ direction ($|S_{12}|^2$) is 94% and 0.9%, respectively, which gives an extinction ratio of 104 (20 dB). Therefore, the metasurface enables a directive source located below the metasurface ($z < 0$) to illuminate an object above the metasurface ($z > 0$). At the same time, reflections from the object will not be seen by any observer below the metasurface. The object can be comprised of an arbitrary material, but should be planar and uniform. This ensures the incident and reflected transverse wavenumbers are identical.

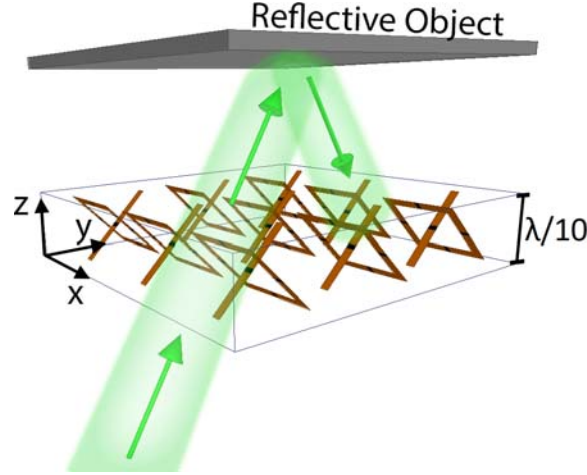


Fig. 3: A metasurface providing unidirectional transmission allows high transmission for obliquely incident plane waves propagating in the $+z$ direction but absorbs radiation propagating in the $-z$ direction.

As mentioned earlier, the transverse momentum of a wavefront incident upon a spatially dispersive metasurface plays the role of a magnetic bias in a nonreciprocal magneto-optic material. The previous examples emulated Faraday rotation and isolation using the transverse momentum of obliquely incident plane waves. However, it is possible to emulate nonreciprocal phenomena at normal incidence as well, as long as the wave carries transverse momentum. For example, vortex beams possess an orbital angular momentum (k_ϕ) that is transverse to the direction of propagation [30]. Thus, these beams provide a self-biasing mechanism that enables nonreciprocal phenomena to be emulated, even when the beam is illuminated at normal incidence.

A metasurface providing unidirectional transmission is designed to work for vortex beams by replacing x , y , and k_y in (6) with r , ϕ , and k_ϕ . Fig. 4 shows full wave simulations of the cross-sections of normally incident vortex beams with topological charge $m = +5$ propagating in the $+z$ and $-z$ directions. The vortex beams are paraxial with $k_\phi/k_0 \approx 0.03$ and $k_z/k_0 \approx 0.999$. In simulation, the computed surface parameters are approximated with a $\lambda_0/5$ thick, lossy and reciprocal material slab with permittivity and permeability given by,

$$\begin{pmatrix} \epsilon_{rr} & \epsilon_{r\phi} & \epsilon_{rz} \\ \epsilon_{\phi r} & \epsilon_{\phi\phi} & \epsilon_{\phi z} \\ \epsilon_{zr} & \epsilon_{z\phi} & \epsilon_{zz} \end{pmatrix} = \begin{pmatrix} \mu_{rr} & \mu_{r\phi} & \mu_{rz} \\ \mu_{\phi r} & \mu_{\phi\phi} & \mu_{\phi z} \\ \mu_{zr} & \mu_{z\phi} & \mu_{zz} \end{pmatrix} = \begin{pmatrix} 1 & 0 & 0 \\ 0 & -1.95 - 0.72j & -0.057 - 0.021j \\ 0 & -0.057 - 0.021j & -0.00045 - 0.00065j \end{pmatrix}. \quad (7)$$

The reflection and transmission coefficients of the thin material slab are virtually identical to those of the ideal metasurface [14]. This permits the use of a commercial electromagnetic solver for simulation, while maintaining the same physical principles and performance. The transmittance through the metasurface is 85% and 0.1% when the vortex beam propagates in the $+z$ and $-z$ directions, respectively. Therefore, the extinction ratio is 710 (28 dB). Since the topological charge of the vortex beam is maintained after reflecting off of an arbitrary homogenous object, the metasurface emulates the response of an isolator that protects the source generating vortex beams from reflections (see Fig. 4(c)). Alternatively, it can be shown through reciprocity that the same metasurface must completely absorb an $m = -5$ order vortex beam that propagates in the $+z$ direction. Therefore, this device filters light based only on its orbital angular momentum and direction of propagation. In contrast, optically active materials (i.e. circular polarizers) filter light based on the spin angular momentum [26, 31, 32].

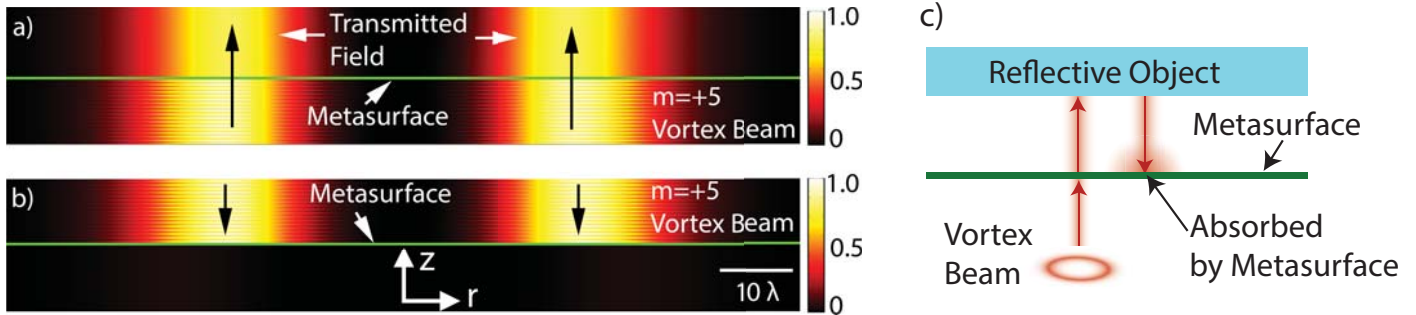


Fig. 4: A metasurface utilizes the orbital angular momentum of a vortex beam to emulate optical isolation. (a) Cross-section through the center of an $m = +5$ vortex beam that is efficiently transmitted through the metasurface when propagating in the $+z$ direction. (b) However, the same vortex beam is absorbed by the metasurface when propagating in the $-z$ direction. (c) The metasurface isolates vortex beam sources located below it from unwanted reflections that might occur due to a reflective object placed above the metasurface. The reflective object should be planar and uniform such that incident waves are reflected towards the specular direction.

In summary, it was shown that metasurfaces supporting longitudinal polarization currents can be modelled with spatially-dispersive 2D surface parameters. These metasurfaces are effectively biased using the transverse momentum of an incident wavefront (i.e. they are self-biased) such that both obliquely incident plane waves and normally incident vortex beams can imitate nonreciprocal phenomena. Spatially dispersive metasurfaces significantly enhance the ability to control electromagnetic wavefronts without resorting to nonreciprocal materials. These metasurfaces will likely impact areas such as antennas [33, 34], angularly selective filters [35], waveguiding surfaces [36], and polarization selective devices [37]. Furthermore, future metasurfaces could be designed to control the evanescent spectrum, or provide additional functionality such as anomalous refraction [38] and beam conversion [39]. Spatially dispersive metasurfaces could also be leveraged to design novel lenses that have tailored transfer functions for plane waves travelling at different angles [40]. It should be noted that spatially dispersive metasurfaces are in general more challenging to fabricate than metasurfaces which only support transverse surface currents. The analysis reported here primarily focused on metasurfaces, rather than bulk materials, because metasurfaces are easier to analyze. However, similar properties are also present in bulk anisotropic materials that are cut along planes rotated relative to their crystal axes. Furthermore, the thickness of a bulk material is an additional degree of freedom that could be exploited to potentially relax fabrication requirements or enhance bandwidth.

ACKNOWLEDGMENTS

This work was funded by the Office of Naval Research (ONR) (N00014-15-1-2390) and NSF Materials Research Science and Engineering Center (MRSEC) (DMR 1120923). The authors would like to thank Dr. Gurkan Gok for insightful discussions on the advantages of adding longitudinal surface currents to metasurfaces.

REFERENCES

- [1] A. M. Mahmoud, A. R. Davoyan, and N. Engheta, "All-passive nonreciprocal metastructure," *Nature Commun.*, vol. 6, p. 8359, 2015.
- [2] Z. Wang, Y. Chong, J. Joannopoulos, and M. Soljačić, "Observation of unidirectional backscattering-immune topological electromagnetic states," *Nature*, vol. 461, pp. 772-775, 2009.
- [3] T. Koderer, D. L. Sounas, and C. Caloz, "Artificial Faraday rotation using a ring metamaterial structure without static magnetic field," *Appl. Phys. Lett.*, vol. 99, p. 031114, 2011.
- [4] N. A. Estep, D. L. Sounas, J. Soric, and A. Alù, "Magnetic-free non-reciprocity and isolation based on parametrically modulated coupled-resonator loops," *Nature Physics*, vol. 10, pp. 923-927, 2014.
- [5] S. Qin, Q. Xu, and Y. E. Wang, "Nonreciprocal Components With Distributedly Modulated Capacitors," *IEEE Trans. on Microwave Theory and Techniques*, vol. 62, pp. 2260-2272, 2014.
- [6] M. Thiel, M. Wegener, and G. von Freymann, "Three-dimensional chiral photonic crystals by direct laser writing," in *MOEMS-MEMS 2008 Micro and Nanofabrication*, San Jose, CA, 2008, pp. 68830K-68830K-6.
- [7] A. B. Khanikaev, S. H. Mousavi, W.-K. Tse, M. Kargarian, A. H. MacDonald, and G. Shvets, "Photonic topological insulators," *Nature Materials*, vol. 12, pp. 233-239, 2013.
- [8] D. W. Berreman, "Optics in stratified and anisotropic media: 4×4 -matrix formulation," *JOSA*, vol. 62, pp. 502-510, 1972.
- [9] L. Barkovskii, G. Borzdov, and A. Lavrinenko, "Fresnel's reflection and transmission operators for stratified gyroanisotropic media," *Journal of Physics A: Mathematical and General*, vol. 20, p. 1095, 1987.
- [10] A. Demetriadou and J. Pendry, "Taming spatial dispersion in wire metamaterial," *Journal of Physics: Condensed Matter*, vol. 20, p. 295222, 2008.
- [11] E. F. Kuester, M. A. Mohamed, M. Piket-May, and C. L. Holloway, "Averaged transition conditions for electromagnetic fields at a metafilm," *IEEE Trans. on Antenn. and Propag.*, vol. 51, pp. 2641-2651, 2003.
- [12] C. L. Holloway, E. F. Kuester, J. A. Gordon, J. O. Hara, J. Booth, and D. R. Smith, "An overview of the theory and applications of metasurfaces: The two-dimensional equivalents of metamaterials," *IEEE Antenn. and Propag. Mag.*, vol. 54, pp. 10-35, 2012.
- [13] C. Pfeiffer and A. Grbic, "Bianisotropic Metasurfaces: Ultra-thin Surfaces for Complete Control of Electromagnetic Wavefronts," *Phys. Rev. Applied*, vol. 113, p. 023902, July 2014.
- [14] A. Shaltout, V. Shalaev, and A. Kildishev, "Homogenization of bi-anisotropic metasurfaces," *Optics Exp.*, vol. 21, pp. 21941-21950, 2013.
- [15] V. Asadchy, Y. Ra'adi, J. Vehmas, and S. Tretyakov, "Functional metamirrors using bianisotropic elements," *Phys. Rev. Lett.*, vol. 114, p. 095503, 2015.
- [16] I. V. Lindell and A. Sihvola, "Electromagnetic boundary and its realization with anisotropic metamaterial," *Phys. Rev. E*, vol. 79, p. 026604, 2009.
- [17] D. Zaluški, S. Hrabar, and D. Muha, "Practical realization of DB metasurface," *Appl. Phys. Lett.*, vol. 104, p. 234106, 2014.
- [18] D. Zaluški, A. Grbic, and S. Hrabar, "Analytical and experimental characterization of metasurfaces with normal polarizability," *Phys. Rev. B*, vol. 93, p. 155156, 2016.
- [19] J. A. Kong, "Theorems of bianisotropic media," *Proc. of the IEEE*, vol. 60, pp. 1036-1046, 1972.
- [20] M. Idemen and A. H. Serbest, "Boundary conditions of the electromagnetic field," *Electronics Lett.*, vol. 23, pp. 704-705, 1987.
- [21] R. F. Harrington, *Time-Harmonic Electromagnetic Fields*. New Jersey: Wiley, 2001.
- [22] See Supplemental Material for additional information on: derivation of updated reciprocity conditions; relations between the 3D surface parameters, 2D surface parameters, material parameters, and scattering parameters; fabrication and measurement procedures; and additional measurements and simulations of the reported metasurfaces.
- [23] A. M. Patel and A. Grbic, "The effects of spatial dispersion on power flow along a printed-circuit tensor impedance surface," *IEEE Trans. on Antenn. and Propag.*, vol. 62, pp. 1464-1469, 2014.
- [24] D. J. Hoppe, Yahya Rahmat-Samii, *Impedance boundary conditions in electromagnetics*: CRC Press, 1995.
- [25] B. H. Fong, J. S. Colburn, J. J. Ottusch, J. L. Visher, and D. F. Sievenpiper, "Scalar and tensor holographic artificial impedance surfaces," *IEEE Trans. on Antenn. and Propag.*, vol. 58, pp. 3212-3221, 2010.

- [26] Y. Zhao, M. Belkin, and A. Alù, "Twisted optical metamaterials for planarized ultrathin broadband circular polarizers," *Nat. Commun.*, vol. 3, p. 870, 2012.
- [27] Y. Ra'di, V. Asadchy, and S. Tretyakov, "One-way transparent sheets," *Phys. Rev. B*, vol. 89, p. 075109, 2014.
- [28] P. F. Goldsmith, "Quasi-optical techniques," *Proceedings of the IEEE*, vol. 80, pp. 1729-1747, 1992.
- [29] B. E. A. Saleh and M. C. Teich, *Fundamentals of Photonics, 2nd Edition*. New Jersey: John Wiley & Sons, Inc., 2007.
- [30] L. Allen, M. W. Beijersbergen, R. Spreeuw, and J. Woerdman, "Orbital angular momentum of light and the transformation of Laguerre-Gaussian laser modes," *Phys. Rev. A*, vol. 45, p. 8185, 1992.
- [31] J. K. Gansel, M. Thiel, M. S. Rill, M. Decker, K. Bade, V. Saile, *et al.*, "Gold Helix Photonic Metamaterial as Broadband Circular Polarizer," *Science*, vol. 325, pp. 1513-1515, Sep 18 2009.
- [32] C. Pfeiffer, C. Zhang, V. Ray, L. J. Guo, and A. Grbic, "High Performance Bianisotropic Metasurfaces: Asymmetric Transmission of Light," *Phys. Rev. Lett.*, vol. 113, p. 023902, 2014.
- [33] C. Pfeiffer and A. Grbic, "Planar Lens-Antennas of Subwavelength Thickness: Collimating Leaky-Waves with Metasurfaces," *IEEE Trans. on Antenn. and Propag.*, vol. 63, pp. 3248-3253, 2015.
- [34] A. Epstein, J. P. S. Wong, and G. V. Eleftheriades, "Cavity-excited Huygens' metasurface antennas for near-unity aperture illumination efficiency from arbitrarily large apertures," *Nature Commun.*, vol. 7, p. 10360, 2016.
- [35] Y. Shen, D. Ye, I. Celanovic, S. G. Johnson, J. D. Joannopoulos, and M. Soljačić, "Optical broadband angular selectivity," *Science*, vol. 343, pp. 1499-1501, 2014.
- [36] A. M. Patel and A. Grbic, "Transformation electromagnetics devices based on printed-circuit tensor impedance surfaces," *IEEE Trans. on Microwave Theory and Techniques*, vol. 62, pp. 1102-1111, 2014.
- [37] T. Niemi, A. Karilainen, and S. Tretyakov, "Synthesis of polarization transformers," *IEEE Trans. on Antenn. and Propag.*, vol. 61, pp. 3102-3111, 2013.
- [38] N. Yu, P. Genevet, M. A. Kats, F. Aieta, J.-P. Tetienne, F. Capasso, *et al.*, "Light propagation with phase discontinuities: generalized laws of reflection and refraction," *Science*, vol. 334, pp. 333-337, 2011.
- [39] C. Pfeiffer and A. Grbic, "Controlling Vector Bessel Beams with Metasurfaces," *Physical Review Applied*, vol. 2, p. 044012, 2014.
- [40] A. Silva, F. Monticone, G. Castaldi, V. Galdi, A. Alù, and N. Engheta, "Performing Mathematical Operations with Metamaterials," *Science*, vol. 343, pp. 160-163, 2014.